

Determination of the band gap and the split-off band in wurtzite GaAs using Raman and photoluminescence excitation spectroscopy

Bernt Ketterer,¹ Martin Heiss,¹ Marie J. Livrozet,¹ Andreas Rudolph,² Elisabeth Reiger,² and Anna Fontcuberta i Morral^{1,*}

¹Laboratoire des Matériaux Semiconducteurs, Institut des Matériaux, Ecole Polytechnique Fédérale de Lausanne, CH-1015 Lausanne, Switzerland

²Institute for Experimental and Applied Physics, University of Regensburg, Universitätsstrasse 31, D-93053 Regensburg, Germany

(Received 25 January 2011; revised manuscript received 16 February 2011; published 21 March 2011)

GaAs nanowires with 100% wurtzite structure are synthesized by the vapor-liquid-solid method in a molecular beam epitaxy system, using gold as a catalyst. We use resonant Raman spectroscopy and photoluminescence to determine the position of the crystal-field split-off band of hexagonal wurtzite GaAs. The temperature dependence of this transition enables us to extract the value at 0 K, which is 1.982 eV. Our photoluminescence excitation spectroscopy measurements are consistent with a band gap of wurtzite GaAs below 1.523 eV.

DOI: [10.1103/PhysRevB.83.125307](https://doi.org/10.1103/PhysRevB.83.125307)

PACS number(s): 78.67.Uh, 61.46.Km, 63.22.-m

I. INTRODUCTION

Nanowires are filamentary crystals with a diameter of the order of a few nanometers. Their increasing importance in both science and engineering is a consequence of the great number of novel experiments and applications they enable.¹⁻⁷ It has been predicted and shown that the reduced diameter of nanowires allows the combination of lattice-mismatched materials when they are fabricated in the nanowire form.^{8,9} The possibility of obtaining new material combinations opens great perspectives in the area of multiple-junction photovoltaics, for example.¹⁰ Recently, an additional degree of freedom in the formation of heterostructures has appeared that concerns the variation of the crystal phase along the nanowire instead of the material composition.¹¹⁻¹³ The degree of control over the crystal phase can be astonishingly accurate depending on the growth method,¹⁴⁻¹⁶ so that perspectives for new device concepts are exciting the nano-science and nanotechnology communities.

While the structural control is becoming increasingly sophisticated, few experimental reports have focused on the details of the electronic structure of wurtzite arsenides or phosphides. Recently, two groups applied photoluminescence excitation (PLE) to determine the valence-band structure of wurtzite InP.^{17,18} The results agreed well with the theoretical expectations. Wurtzite GaAs has been shown to be more controversial. First, there are significant disagreements between the theoretical calculations of the band gap.^{19,20} Second, luminescence studies of different groups have shown results consistent with a band gap of 1.54,²¹ 1.522,²² and 1.50 eV.²³⁻²⁵ The apparent lack of agreement between the various groups might be explained by the fact that the optical and structural characterizations were not performed on exactly the same nanowire. Recently, we designed an experiment in which both the luminescence and electron microscopy measurements were realized on the identical nanowire.²⁵ We investigated nanowires presenting either a mixture of wurtzite and zinc-blende phases or 100% wurtzite crystal phase. These and previous experiments were consistent with a band gap of 1.50 eV for wurtzite GaAs.^{24,25}

As a consequence of the hexagonal symmetry, it has been shown that the band structure of wurtzite semiconductors exhibits important differences compared to the band structure

of the respective zinc-blende (cubic) counterparts.¹⁹ In Fig. 1 we compare the band structure of zinc-blende and wurtzite GaAs close to the Γ point according to recent theoretical results from De and Pryor.¹⁹ As a consequence of the zone folding induced by the doubling of the unit cell along the (111) direction, an additional conduction band with Γ_8 symmetry appears for the wurtzite structure. In contrast to other III-V semiconductors, the energy separation Δ_{CB} between these two conduction bands is expected to be the smallest for the case of wurtzite GaAs. The theoretical predicted values of $\Delta_{CB} = -23$ meV (Ref. 20), $\Delta_{CB} = +85$ meV (Ref. 19), or $\Delta_{CB} = +87$ meV (Ref. 25) are even smaller than the predicted splitting of the two uppermost valence bands. There, the crystal-field splitting and spin-orbit interaction lift the degeneracy of the heavy- and light-hole states for the wurtzite structure.^{19,26} Furthermore a crystal-field split-off hole (CH) band is predicted further down in energy below the valence-band edge compared to the split-off band in zinc-blende GaAs.¹⁹ To the best of our knowledge, there are no studies to date providing the values of either the crystal-field splitting or split-off band for the case of wurtzite GaAs.

Luminescence studies allow the probing of transitions between the conduction-band minimum and the highest-energy valence-band states. In order to obtain information on the valence-band structure (i.e., crystal-field and split-off band splitting) other types of experiments such as photoluminescence excitation and resonant Raman scattering should be implemented.^{17,27-29} In this paper we use resonant Raman scattering and photoluminescence excitation spectroscopy to probe the crystal-field split-off valence band to conduction-band transition and to provide more clarity and consistency in recent luminescence studies that attribute the band gap of wurtzite to be at 1.50 eV.

II. EXPERIMENTAL DETAILS

Wurtzite GaAs nanowires were grown by the Au-catalyzed vapor-liquid-solid method on GaAs (111)*B* substrates at a growth temperature of 540 °C under an As₄ beam flux of 1.27×10^{-6} Torr at a Ga rate equivalent to a planar growth of 0.4 Å/s. The growth time was 4 h. The nucleation and growth followed the vapor-liquid-solid mechanism, with Au

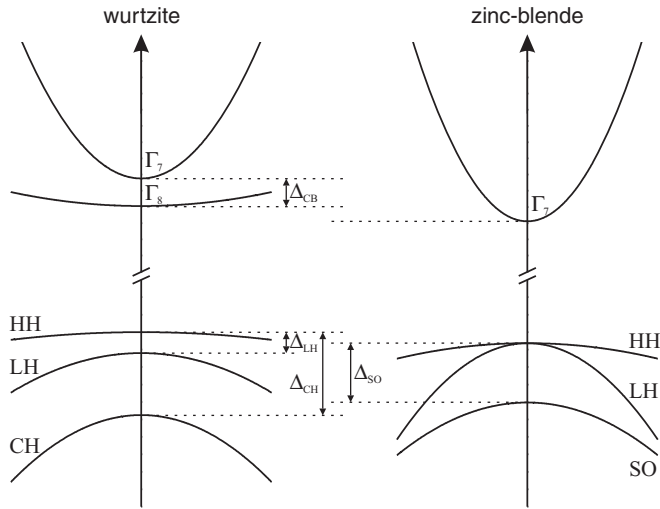


FIG. 1. (Left) Schematic band diagram for wurtzite GaAs near the Brillouin zone center according to Ref. 19. (Right) Schematic band diagram for zinc-blende GaAs near the Brillouin zone center.

as catalyst.³⁰ Details of the growth procedure are described in Ref. 31. After the axial growth of the nanowires, the growth parameters were changed to conditions suitable for planar growth and the nanowires were passivated by an epitaxial prismatic shell of AlGaAs/GaAs material.³² The two-dimensional (2D) equivalent amount grown during capping was 60 nm AlGaAs followed by 30 nm GaAs. The total diameter of the nanowires is approximately 85 nm. The structure was shown to be 100% wurtzite with a few twin planes.²⁵

Single-nanowire spectroscopy was realized on nanowires dispersed on a marked silicon substrate. In the Raman spectroscopy experiments, the nanowires were photoexcited by Ar⁺Kr⁺ or HeNe lasers with wavelengths of 647.1 and 632.8 nm, respectively. In the photoluminescence excitation spectroscopy measurements, the excitation source was a Koheras SuperK supercontinuum source filtered by an acousto-optical tunable filter (AOTF). During the PLE measurement the actual power of the excitation light was kept constant throughout the entire wavelength range by means of a computer-controlled feedback loop. In both the Raman and PLE spectroscopy experiments, the light was focused to a submicrometer spot using a cover-glass-corrected microscope objective with 0.75 numerical aperture. The measurements were realized at a temperature between 10 and 360 K in a liquid-helium-flow cryostat. The scattered light was collected through the same objective and focused on the entrance slit of a triple spectrometer and the spectrum collected thanks to a Peltier-cooled charge-coupled device.

III. RESULTS

A. Resonant Raman scattering

We first present the resonant Raman scattering experiment. Here, we look for the conditions leading to sharp resonances of the first- and second-order LO phonons that occur via the dipole-forbidden Fröhlich electron-phonon interaction.^{34,35} The resonance is observed when the excitation energy coincides with an interband critical point E_c in the joint density of

states of the semiconductor. In our case, we reach the transition between the split-off valence band and the conduction band. Typical Raman spectra of wurtzite GaAs obtained in polarized configuration with the incident and detected polarization parallel to the c axis, which lies along the nanowire axis, are shown in Fig. 2(a). This configuration is denoted as $x(z,z)\bar{x}$ in Porto notation. We plot the spectra under nonresonant and resonant conditions, the difference being the intensity of the LO and second-order (2LO) peaks. Under nonresonant conditions, only the $A_1(\text{TO})$ mode at $\sim 270 \text{ cm}^{-1}$ is allowed in $x(z,z)\bar{x}$ configuration.^{36,37} Under resonant conditions, not only does the intensity of the dipole-forbidden $A_1(\text{LO})$ mode at $\sim 290 \text{ cm}^{-1}$ increase significantly, but also the second-order Raman scattering by two $A_1(\text{LO})$ phonons at $\sim 580 \text{ cm}^{-1}$ is strongly enhanced.³⁸ For simplicity, in the following we will denominate the $A_1(\text{TO})$ and $A_1(\text{LO})$ modes as simply TO and LO.

Now we proceed with the determination of the resonance Raman conditions for the measurement of the critical points of wurtzite GaAs. We measured the Raman spectra of single wurtzite GaAs nanowires as a function of the excitation energy and temperature. Other methods to tune the band-gap energy with respect to the laser energy concern the use of a tunable laser or the application of pressure.³⁴ The excitation wavelengths used were 632.8 and 647.1 nm. The temperature was varied between 10 and 360 K. The intensity of the LO and 2LO peaks normalized to the intensity of the TO mode as a function of temperature for the excitations at 632.8 and 647.1 nm is shown in Figs. 2(b) and 2(c), respectively. The resonance profile of the LO-phonon scattering shows a single maximum under outgoing resonance, where the scattered light exactly matches a gap of the electronic band structure. The 2LO-phonon scattering reveals a strong outgoing resonance ($E_{\text{laser}} = E_c + \hbar\omega_{2\text{LO}}$) as well as a weaker intermediate resonance ($E_{\text{laser}} = E_c + \hbar\omega_{\text{LO}}$). No incoming resonance is observed for either the LO or the 2LO scattering. This behavior has also been observed for zinc-blende GaAs.³⁴ For the excitation at 632.8 nm, we observe the strongest resonance of the LO and 2LO peaks at 197 and 255 K, respectively. For the excitation at 647.1 nm, we observe it at 282 and 327 K. For these temperatures, the energy of the critical point E_c is then calculated:

$$E_c + \hbar\omega_{\text{ph}} = hc/\lambda, \quad (1)$$

where ω_{ph} corresponds to the frequency of the phonons (LO or 2LO) and λ is the excitation wavelength. For the temperatures of 197, 255, 282, and 327 K under which the resonances occur, we obtain critical energies of 1.925, 1.889, 1.882, and 1.846 eV, respectively. These points are reported in Fig. 2(d). Limitations in available wavelengths do not allow us to obtain the energy of this transition at lower temperatures. Nevertheless, we have tried to measure direct luminescence from the recombination between the two resonant levels. Because there are very few unoccupied states in the CH split-off band, such a transition is extremely weak. We have obtained luminescence of this transition for an incident polarization parallel to the hexagonal c axis at temperatures between 10 and 40 K by exciting with 568.2 nm and a power of 50 μW . The acquisition time was 30 min, which is between three and four orders of magnitude longer than our typical luminescence experiments in our nanowires for equivalent excitation powers. The spectra are

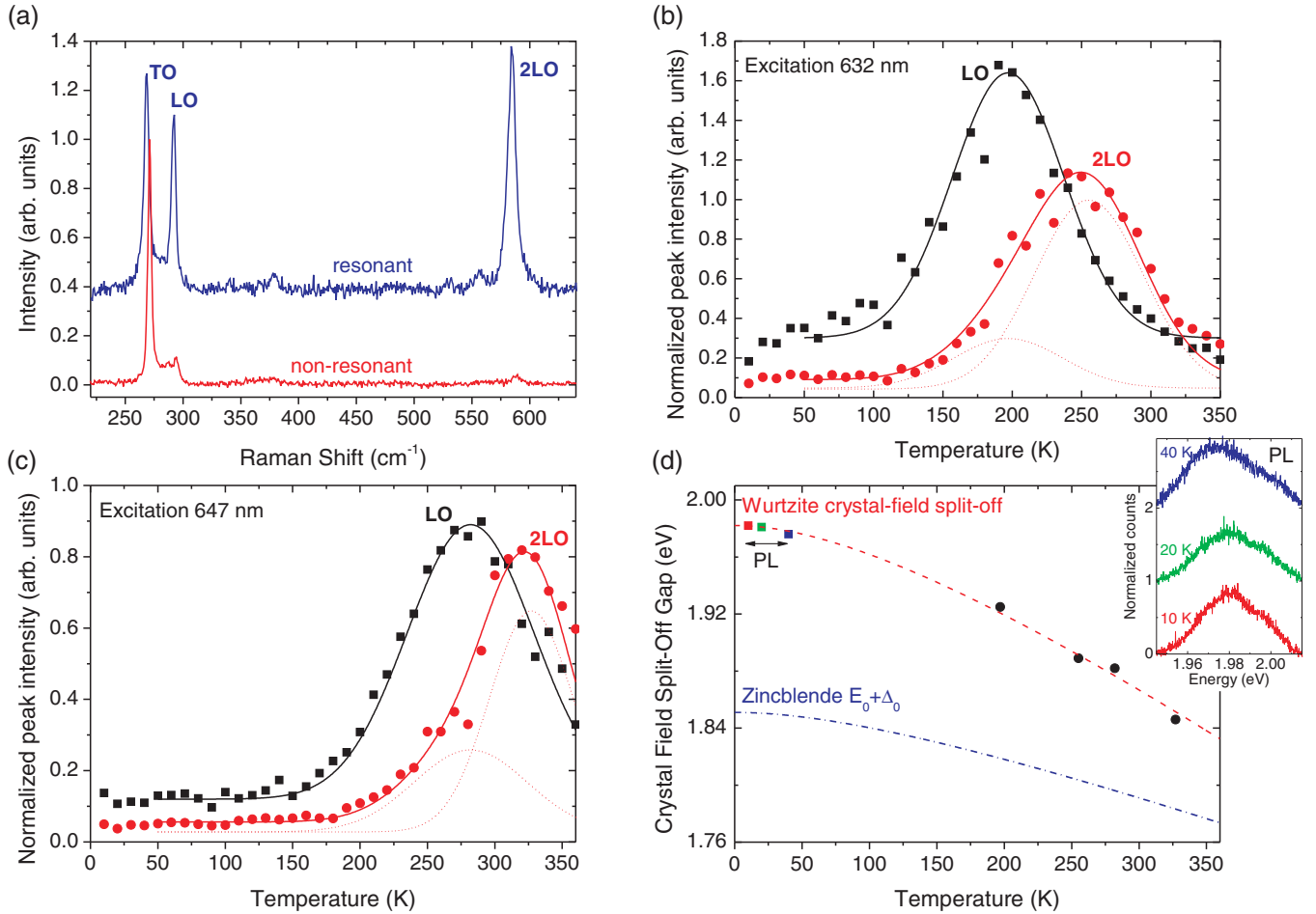


FIG. 2. (Color online) (a) Raman spectra of individual wurtzite GaAs nanowires at LO (2LO) resonance and out of resonance. (b) and (c) show LO and 2LO resonance profiles for 632.8 and 647.1 nm excitation. The LO-phonon scattering exhibits a single maximum under outgoing resonance. The 2LO resonance profile consists of a strong outgoing resonance ($E_{\text{laser}} = E_c + \hbar\omega_{2\text{LO}}$) and a weaker intermediate resonance ($E_{\text{laser}} = E_c + \hbar\omega_{\text{LO}}$). (d) Temperature-dependent variation of the crystal-field split-off gap in wurtzite GaAs with a fit to the Varshni equation. The inset shows the measured photoluminescence (PL) from this gap at three different temperatures. The temperature dependence of the zinc-blende $E_0 + \Delta_0$ gap (Ref. 33) is shown for comparison.

shown in the inset of Fig. 2(d). At temperatures of 10, 20, and 40 K we observe PL centered at 1.982, 1.981, and 1.976 eV, respectively. This enables us to complete the curve of the temperature dependence. The temperature-dependent variation of the band-gap energy can be commonly given in terms of the α and β coefficients of the Varshni equation:³⁹

$$E_c(T) = E_c(0) - \frac{\alpha T^2}{T + \beta}. \quad (2)$$

Least-squares fitting to the experimental data [the result is shown in Fig. 2(d)] gives the fitting parameters α and β as 6.9×10^{-4} eV/K and 245.8 K, respectively. For $T = 0$ K we find a gap energy of $E_c(0) = 1.982$ eV. We now discuss the nature of the extrapolated interband critical point $E_c(T = 0) = 1.982$ eV in wurtzite GaAs. It should be pointed out that we are reporting the direct values and quantum confinement is not considered. The quantum confinement for the fundamental transition in these nanowires should be in the order of ~ 15 meV.²⁵ In zinc-blende GaAs, the interband transition from the spin-orbit-split valence band to the lowest

conduction band at the Γ point $E_0 + \Delta_0$ is found³³ at 1.851 eV for $T = 0$ K [see Fig. 2(d)]. Likewise, we attribute the observed energy gap in wurtzite GaAs to a transition from the crystal-field split-off valence band to one of the lowest-energy conduction bands at the Γ point of the Brillouin zone. For the discussion, we need to come back to Fig. 1. The crystal-field split-off valence band is labeled with CH. This band has a Γ_7 symmetry. In the conduction band there is an important difference with respect to zinc blende. There is the first minimum labeled Γ_8 , which originates from the zone-folded L valleys of zinc-blende GaAs. This band is separated by a small energy fraction Δ_{CB} from a close-lying conduction band with Γ_7 symmetry. According to the selection rules in materials with hexagonal wurtzite structure, optical transitions from the Γ_{7v} CH valence band to the Γ_{7c} conduction band are dipole allowed. Transitions from the Γ_{7v} valence band to the Γ_{8c} conduction band are dipole forbidden.⁴⁰ Generally, these selection rules may be softened in resonant Raman exciting conditions,⁴¹ meaning that resonant Raman scattering from an optically forbidden transition cannot be completely excluded.

However, the fact that we observe photoluminescence from this energy gap lets us conclude that the transition should be the dipole-allowed CH (Γ_{7v}) to Γ_{7c} . Consequently, we assign the observed critical point with energy of 1.982 eV in wurtzite GaAs to the interband transition from the crystal-field split-off valence band to the second lowest conduction band. Finally, we compare the experimental findings with theoretical predictions. Based on an empirical pseudopotential method including spin-orbit coupling, De and Pryor calculated values of 1.978 and 2.063 eV, respectively, for the Γ_{7v} - Γ_{8c} and Γ_{7v} - Γ_{7c} interband transitions. This means that our experiment agrees with this theory within 4% (81 meV).

B. Photoluminescence excitation spectroscopy

For a further understanding of the band structure of wurtzite GaAs, photoluminescence excitation spectroscopy was realized. A typical PL spectrum of a single nanowire is shown in Fig. 3(a). A single peak centered at 1.515 eV is observed, consistent with our previous works.²⁵ The excitation spectroscopy measurements were realized by detecting the integrated intensity of the emission as a function of the excitation energy. The resulting PLE measurements on single nanowires are shown in Fig. 3(a). We start by describing the measurements realized at high photon energies of the excitation light, between 1.58 and 2.25 eV, shown in Fig. 3(a). One should note that the gap 1.8–1.9 eV between the two PLE measurements is a result of switching between two AOTFs with disjoint output ranges. The power density for these measurements was of the order of 300 W/cm². We observe a relatively sharp increase in the signal at ~ 1.6 eV and a peak centered at ~ 2 eV. The latter is consistent with the Raman measurements that detect the band gap plus split-off band transition close to 2 eV at 10 K. One should note that the decrease of PL intensity at higher energies is also reinforced by the decrease of the penetration depth of the excitation. We believe the increased signal at ~ 1.6 eV comes from a contribution of the Al_{0.33}Ga_{0.67}As shell, which exhibits about 2.7 times the volume of the nanowire core in the present sample. The electron-hole pairs generated in the shell can diffuse and recombine with the wurtzite GaAs core, thereby contributing to the PLE signal. The band gap of wurtzite AlAs is theoretically expected to be significantly smaller compared to the (indirect-band-gap) zinc-blende counterpart as a result of the zone folding along the Γ - L direction.^{19,20} A recombination around 1.6 eV is consistent with recent measurements on wurtzite Al_xGa_{1-x}As with comparable nominal composition.⁴² In principle this transition could also be in reasonable agreement with a transition from the heavy-hole band to the second conduction band with Γ_7 symmetry that is predicted at 1.588 eV, and even with a transition from the Γ_{7v} light-hole band to the Γ_{8c} conduction band (1.623 eV).¹⁹ However, according to theory, the transition Γ_{7v} - Γ_{8c} should not be dipole allowed⁴⁰ and, furthermore, the transitions related to the light-hole band or the Γ_7 conduction band should be weak due to the smaller joint density of states.¹⁹ We therefore believe that the increase in PLE signal around 1.6 eV signal is predominantly caused by the onset of absorption in the wurtzite Al_{0.33}Ga_{0.67}As shell.

Finally, we turn our attention to PLE measurements realized closer to the band gap. In order to approach the band gap with

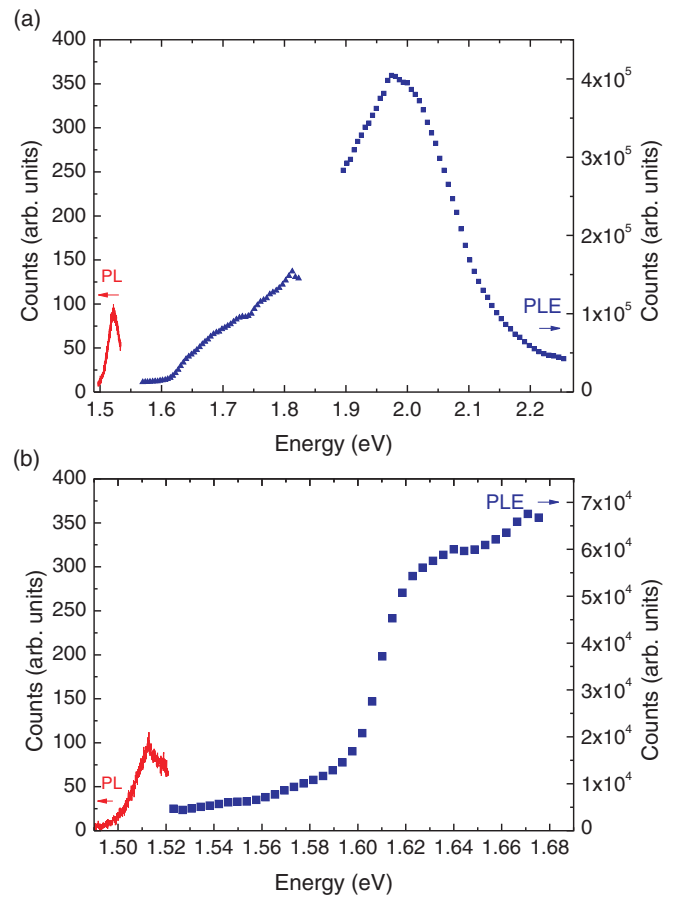


FIG. 3. (Color online) (a) Integrated PLE signal data points obtained on single nanowires. The blue triangles and blue squares correspond to separate experiments on different single nanowires. The signal is normalized for continuity around 1.8–1.9 eV. The red curve corresponds to the PL signal obtained for excitation with a photon energy of 1.726 eV. (b) Integrated PLE data of a nanowire ensemble (blue squares). The red line shows the corresponding photoluminescence spectrum for an excitation photon energy of 1.527 eV.

the excitation source, the spectral output of the AOTF had to be further narrowed by passing the excitation light through a monochromator ($f = 300$ mm; grating, 150 grooves mm) and subsequently projecting the light from the exit slit of this monochromator to the sample. This enabled us to narrow down the linewidth below 1 nm and to remove the remaining background emission from the AOTF. This further step also limited the maximum excitation power density down to about 10 W/cm². As a consequence, the collected signal was significantly reduced with respect to the measurements for excitation energies higher than 1.6 eV. In order to increase the signal-to-noise ratio for the energy range between 1.525 and 1.68 eV, we realized measurements on nanowire ensembles. As shown in Fig. 3(b), the PL spectrum of the ensemble is extremely similar to that of single nanowires. This is possible because all nanowires present the identical structure. Consistent with the measurements at higher excitation energies, we observe an increase in PLE intensity around 1.6 eV. For energies below 1.6 eV and down to 1.523 eV, no other clearly resolvable PLE feature is observed. One should note that the PL

spectrum shown in Fig. 3(b) corresponds to the one obtained at the excitation energy of 1.527 eV. We therefore estimate the Stokes shift—the energy offset between the emission peak and the onset of absorption—to be smaller than 10 meV. From our PLE measurements we can estimate an upper limit for the band gap of wurtzite GaAs as 1.523 eV. As we have discussed in detail previously,²⁵ taking into account quantum confinement effects, the emission peak is in reasonable agreement with the predictions of De and Pryor of a bulk wurtzite band gap of 1.503 eV.¹⁹ At the same time, our PLE data are inconsistent with a band gap of 1.552 eV as predicted by Murayama and Nakayama,²⁰ as no feature is observed in the corresponding spectral region.

IV. CONCLUSIONS

In conclusion, we have measured the position of the crystal-field split-off band of wurtzite GaAs by resonant

Raman and photoluminescence spectroscopy. The temperature dependence was fitted with the Varshni equation and the parameters were extracted. A value of 1.982 eV was obtained for the CH split-off to conduction band transition at 0 K. PLE measurements down to 1.525 eV are consistent with a band gap of wurtzite GaAs below 1.523 eV and inconsistent with a transition at 1.55 eV.

ACKNOWLEDGMENTS

The authors thank D. Schuh for assisting with the experiment. We are grateful for financial support from the Swiss National Science Foundation through Grants No. 2000021-121758/1 and No. 129775/1 and by the European Research Council under Upcon grantâ. E.R. acknowledges financial support from the European Research Area Nanoscience Project QOptInt. E.R. and A.R. are grateful for support via SFB 689.

*anna.fontcuberta-morral@epfl.ch

¹F. Qian, Y. Li, S. Gradečak, H.-G. Park, Y. Dong, Y. Ding, Z. L. Wang, and C. M. Lieber, *Nature Mater.* **7**, 701 (2008).

²F. Qian, Y. Li, S. Gradečak, D. Wang, C. J. Barrelet, and C. M. Lieber, *Nano Lett.* **4**, 1975 (2004).

³J. Xiang, W. Lu, Y. Hu, Y. Wu, H. Yan, and C. M. Lieber, *Nature (London)* **441**, 489 (2006).

⁴A. B. Greytak, C. J. Barrelet, Y. Li, and C. M. Lieber, *Appl. Phys. Lett.* **87**, 151103 (2005).

⁵B. Fluegel, A. Mascarenhas, D. W. Snoke, L. N. Pfeiffer, and K. West, *Nature Photon.* **1**, 701 (2007).

⁶K. W. J. Barnham and G. Duggan, *J. Appl. Phys.* **67**, 3490 (1990).

⁷G. Ferrari, G. Goldoni, A. Bertoni, G. Cuoghi, and E. Molinari, *Nano Lett.* **9**, 1631 (2009).

⁸F. Glas, *Phys. Rev. B* **74**, 121302 (2006).

⁹T. Mårtensson, C. P. T. Svensson, B. A. Wacaser, M. W. Larsson, W. Seifert, K. Deppert, A. Gustafsson, L. R. Wallenberg, and L. Samuelson, *Nano Lett.* **4**, 1987 (2004).

¹⁰J. Wallentin, J. M. Persson, J. B. Wagner, L. Samuelson, K. Deppert, and M. T. Borgström, *Nano Lett.* **10**, 974 (2010).

¹¹M. Mattila, T. Hakkarainen, M. Mulot, and H. Lipsanen, *Nanotechnology* **17**, 1580 (2006).

¹²A. Mishra, L. V. Titova, T. B. Hoang, H. E. Jackson, L. M. Smith, J. M. Yarrison-Rice, Y. Kim, H. J. Joyce, Q. Gao, H. H. Tan, and C. Jagadish, *Appl. Phys. Lett.* **91**, 263104 (2007).

¹³J. L. Birman, *Phys. Rev. Lett.* **2**, 157 (1959).

¹⁴R. E. Algra, M. A. Verheijen, M. T. Borgstrom, L.-F. Feiner, G. Immink, W. J. P. van Enckevort, E. Vlieg, and E. P. A. M. Bakkers, *Nature (London)* **456**, 369 (2008).

¹⁵P. Caroff, K. A. Dick, J. Johansson, M. E. Messing, K. Deppert, and L. Samuelson, *Nature Nanotechnol.* **4**, 50 (2009).

¹⁶K. A. Dick, C. Thelander, L. Samuelson, and P. Caroff, *Nano Lett.* **10**, 3494 (2010).

¹⁷S. Perera, K. Pemasiri, M. A. Fickenscher, H. E. Jackson, L. M. Smith, J. Yarrison-Rice, S. Paiman, Q. Gao, H. H. Tan, and C. Jagadish, *Appl. Phys. Lett.* **97**, 023106 (2010).

¹⁸E. G. Gadret, G. O. Dias, L. C. O. Dacal, M. M. de Lima, C. V. R. S. Ruffo, F. Iikawa, M. J. S. P. Brasil, T. Chiamonte, M. A. Cotta, L. H. G. Tizei, D. Ugarte, and A. Cantarero, *Phys. Rev. B* **82**, 125327 (2010).

¹⁹A. De and C. E. Pryor, *Phys. Rev. B* **81**, 155210 (2010).

²⁰M. Murayama and T. Nakayama, *Phys. Rev. B* **49**, 4710 (1994).

²¹T. B. Hoang, A. F. Moses, H. L. Zhou, D. L. Dheeraj, B. O. Fimland, and H. Weman, *Appl. Phys. Lett.* **94**, 133105 (2009).

²²F. Martelli, M. Piccin, G. Bais, F. Jabeen, S. Ambrosini, S. Rubini, and A. Franciosi, *Nanotechnology* **18**, 125603 (2007).

²³M. Moewe, L. C. Chuang, S. Crankshaw, C. Chase, and C. Chang-Hasnain, *Appl. Phys. Lett.* **93**, 023116 (2008).

²⁴D. Spirkoska, J. Arbiol, A. Gustafsson, S. Conesa-Boj, F. Glas, I. Zardo, M. Heigoldt, M. H. Gass, A. L. Bleloch, S. Estrade, M. Kaniber, J. Rossler, F. Peiro, J. R. Morante, G. Abstreiter, L. Samuelson, and A. Fontcuberta i Morral, *Phys. Rev. B* **80**, 245325 (2009).

²⁵M. Heiss, S. Conesa-Boj, J. Ren, H.-H. Tseng, A. Gali, A. Rudolph, E. Uccelli, F. Peiró, J. R. Morante, D. Schuh, E. Reiger, E. Kaxiras, J. Arbiol, and A. Fontcuberta i Morral, *Phys. Rev. B* **83**, 045303 (2011).

²⁶S. L. Chuang and C. S. Chang, *Phys. Rev. B* **54**, 2491 (1996).

²⁷M.-E. Pistol, M. Gerling, D. Hessman, and L. Samuelson, *Phys. Rev. B* **45**, 3628 (1992).

²⁸N. Sköld, M.-E. Pistol, K. A. Dick, C. Pryor, J. B. Wagner, L. S. Karlsson, and L. Samuelson, *Phys. Rev. B* **80**, 041312 (2009).

²⁹J. M. Calleja and M. Cardona, *Phys. Rev. B* **16**, 3753 (1977).

³⁰R. S. Wagner and W. C. Ellis, *Appl. Phys. Lett.* **4**, 89 (1964).

³¹A. Rudolph, M. Soda, M. Kiessling, T. Wojtowicz, D. Schuh, W. Wegscheider, J. Zweck, C. Back, and E. Reiger, *Nano Lett.* **9**, 3860 (2009).

³²A. Fontcuberta i Morral, D. Spirkoska, J. Arbiol, M. Heigoldt, J. R. Morante, and G. Abstreiter, *Small* **4**, 899 (2008).

³³P. Lautenschlager, M. Garriga, S. Logothetidis, and M. Cardona, *Phys. Rev. B* **35**, 9174 (1987).

³⁴R. Trommer and M. Cardona, *Phys. Rev. B* **17**, 1865 (1978).

- ³⁵W. Kauschke, M. Cardona, and E. Bauser, *Phys. Rev. B* **35**, 8030 (1987).
- ³⁶I. Zardo, S. Conesa-Boj, F. Peiro, J. R. Morante, J. Arbiol, E. Uccelli, G. Abstreiter, and A. Fontcuberta i Morral, *Phys. Rev. B* **80**, 245324 (2009).
- ³⁷S. Crankshaw, L. C. Chuang, M. Moewe, and C. Chang-Hasnain, *Phys. Rev. B* **81**, 233303 (2010).
- ³⁸M. Brewster, O. Schimek, S. Reich, and S. Gradečak, *Phys. Rev. B* **80**, 201314 (2009).
- ³⁹Y. P. Varshni, *Physica* **34**, 149 (1967).
- ⁴⁰P. Tronc, Y. Kitaev, G. Wang, M. Limonov, A. Panfilov, and G. Neu, *Phys. Status Solidi B* **216**, 599 (1999).
- ⁴¹R. Martin and L. Falicov, in *Light Scattering in Solids I*, Topics in Applied Physics Vol. 8 (Springer, Berlin, 1983), pp. 79–145.
- ⁴²H. L. Zhou, T. B. Hoang, D. L. Dheeraj, A. T. J. van Helvoort, L. Liu, J. C. Harmand, B. O. Fimland, and H. Weman, *Nanotechnology* **20**, 415701 (2009).